

Task 2 - Research Civil Aircraft Model (RCAM)

Caleth Sebastián Carrillo Grijalba / 000480692
Miguel Angel Rendón Hoyos / 000486701

November 10, 2025

Objective

The objective of this task is to design and implement a simplified simulation of the **Research Civil Aircraft Model (RCAM)** using Python. The simulation integrates the aircraft's nonlinear equations of motion, computes aerodynamic forces and moments, and visualizes the evolution of the nine state variables for different control scenarios. The study aims to understand the dynamic response of a large transport-type aircraft under normal flight, control input perturbations, and asymmetric thrust conditions.

1 Backend: Model Equations and Implementation

1. State definition

The aircraft state vector is defined as:

$$X = [u \ v \ w \ p \ q \ r \ \phi \ \theta \ \psi]^\top$$

where (u, v, w) are the body-axis velocity components, (p, q, r) the angular rates, and (ϕ, θ, ψ) the Euler angles (roll, pitch, yaw).

2. Control inputs

$$U = [\delta_a \ \delta_e \ \delta_r \ \delta_{t1} \ \delta_{t2}]^\top$$

representing aileron, stabilator, rudder, and throttle commands for the left and right engines.

3. Aircraft constants

The nominal constants of the model correspond to a large transport aircraft:

$$\begin{aligned} m &= 120,000 \text{ kg}, & S &= 260 \text{ m}^2, & \bar{c} &= 6.6 \text{ m}, \\ l_t &= 24.8 \text{ m}, & S_t &= 64 \text{ m}^2, & g &= 9.81 \text{ m/s}^2. \end{aligned}$$

The center of gravity and aerodynamic center are located at:

$$(X_{cg}, Y_{cg}, Z_{cg}) = (0.23c_{bar}, 0, 0.10c_{bar}), \quad (X_{ac}, Y_{ac}, Z_{ac}) = (0.12c_{bar}, 0, 0).$$

4. Aerodynamic coefficients

The aerodynamic coefficients are functions of the angle of attack (α), sideslip (β), and control inputs.

Lift coefficient (C_L):

$$C_L = \begin{cases} n(\alpha - \alpha_{L0}) & \text{if } \alpha \leq \alpha_{switch} \\ a_3\alpha^3 + a_2\alpha^2 + a_1\alpha + a_0 & \text{otherwise} \end{cases} + 3.1 \frac{S_t}{S} \alpha_t$$

where $\alpha_t = \alpha - \varepsilon + \delta_e + 1.3ql_t/V_a$, and $\varepsilon = \frac{d\varepsilon}{d\alpha}(\alpha - \alpha_{L0})$.

Drag and side-force coefficients:

$$C_D = 0.13 + 0.07(n\alpha + 0.654)^2, \quad C_Y = -1.6\beta + 0.24\delta_r$$

5. Aerodynamic forces in body axes

Using the dynamic pressure $Q = \frac{1}{2}\rho V_a^2$:

$$\mathbf{F}_A^s = \begin{bmatrix} -C_D Q S \\ C_Y Q S \\ -C_L Q S \end{bmatrix}, \quad \mathbf{F}_A^b = C_{bs} \mathbf{F}_A^s$$

where C_{bs} is the transformation matrix from stability to body axes.

6. Aerodynamic moments

The aerodynamic moment about the aerodynamic center is computed as:

$$\mathbf{M}_{A,ac}^b = C_{M,ac}^b Q S c_{bar} \quad \text{where} \quad C_{M,ac}^b = \eta + \frac{c_{bar}}{V_a} D_{CM_x} \boldsymbol{\omega}_b + D_{CM_u} \mathbf{U} \quad (1)$$

with η containing cross-coupling terms proportional to β and α .

7. Total forces and moments

$$\mathbf{F}_b = \mathbf{F}_g + \mathbf{F}_E + \mathbf{F}_A, \quad \mathbf{M}_b = \mathbf{M}_{A,cg} + \mathbf{M}_{E,cg}$$

where:

- \mathbf{F}_E is the thrust from both engines, proportional to throttle inputs.
- $\mathbf{F}_g = m\mathbf{g}_b$ represents gravity in the body frame.
- $\mathbf{M}_{A,cg}$ and $\mathbf{M}_{E,cg}$ are the aerodynamic and engine moments about the center of gravity.

8. Equations of motion

$$\dot{\mathbf{v}}_b = \frac{1}{m} \mathbf{F}_b - \boldsymbol{\omega}_b \times \mathbf{v}_b \quad \dot{\boldsymbol{\omega}}_b = I_b^{-1} (\mathbf{M}_b - \boldsymbol{\omega}_b \times (I_b \boldsymbol{\omega}_b)) \quad \begin{bmatrix} \dot{\phi} \\ \dot{\theta} \\ \dot{\psi} \end{bmatrix} = H_\phi \boldsymbol{\omega}_b \quad (2)$$

where I_b is the inertia tensor and H_ϕ the Euler kinematic transformation matrix.

9. Numerical integration

The system is integrated with a 4th-order Runge–Kutta (RK4) method:

$$X_{k+1} = X_k + \frac{\Delta t}{6} (k_1 + 2k_2 + 2k_3 + k_4)$$

where $k_i = f(X_i, U_i, \rho)$, with $\Delta t = 0.01$ s for internal integration and results sampled every 0.5 s.

2 Key Observations from Test Cases

Figures 1–3 present the evolution of the nine state variables for each test case. The results are consistent with the expected physical response of an aircraft.

Case 1 - base flight

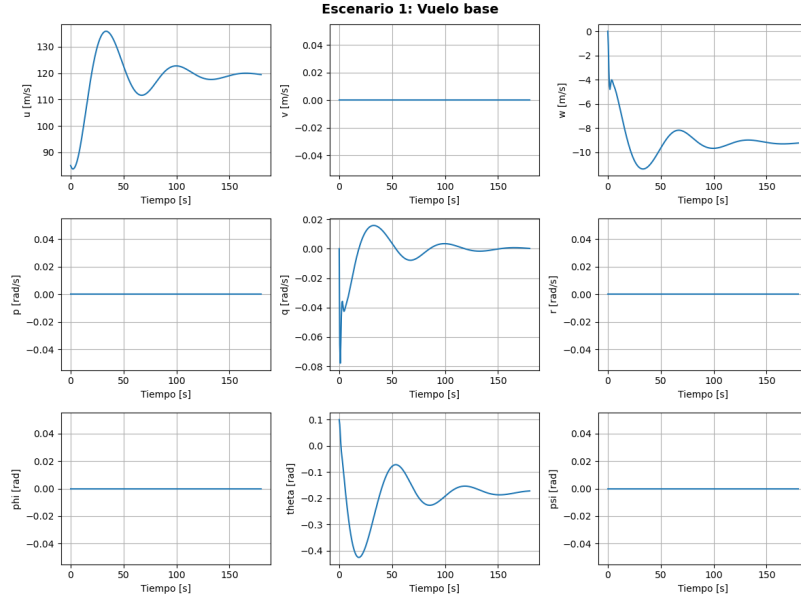


Figure 1: Case 1: Steady flight – state evolution.

In this scenario, the aircraft begins in a trimmed steady–flight condition with small attitude and control deflections. The results show that the longitudinal dynamics dominate the response, particularly the translational velocities u , v , and w .

- **Longitudinal velocity (u):** It initially decreases slightly due to the balance between thrust and drag, then rises sharply as the aerodynamic forces adjust, exhibiting a damped oscillation typical of the *phugoid mode*. The oscillations gradually diminish as the aircraft reaches a new equilibrium near 115–120 m/s.
- **Lateral velocity (v):** It remains nearly zero throughout the simulation, confirming that the motion is symmetric and there are no lateral disturbances.
- **Vertical velocity (w):** It shows a negative transient (downward motion), followed by small oscillations that correspond to pitch adjustments during the phugoid response.

Regarding the angular rates:

- p and r remain close to zero, consistent with symmetric flight (no roll or yaw motion).
- q exhibits small oscillations linked to the longitudinal short–period and phugoid modes.

Finally, for the Euler angles:

- ϕ and ψ stay near zero, as expected for straight flight without lateral deviation.
- θ shows an oscillatory pattern that mirrors the variations in u and w , indicating pitch adjustments that stabilize the lift–weight balance.

Case 2 — Aileron pulse ($+5^\circ$ at $t = 30\text{ s}$).

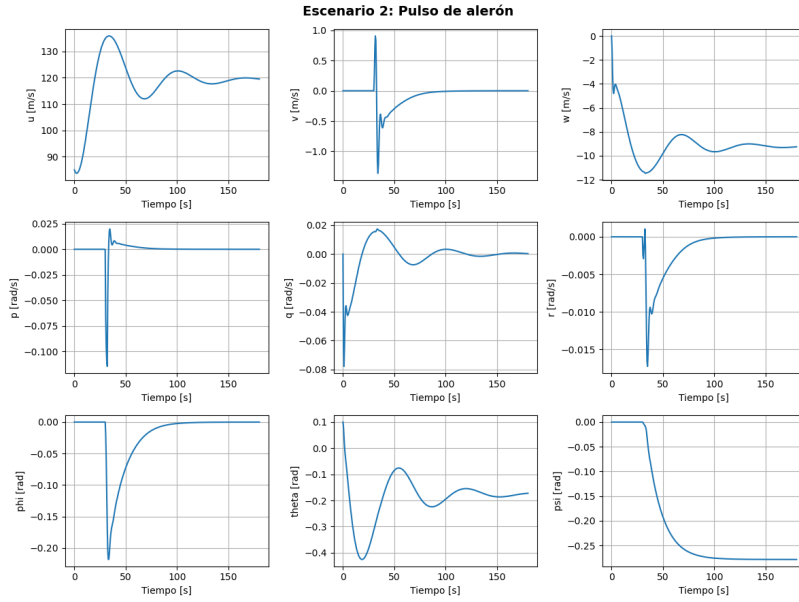


Figure 2: Case 2: Aileron pulse ($+5^\circ$ at 30 s).

In this case, a temporary aileron deflection of $+5^\circ$ is applied at $t = 30\text{ s}$ for 2 seconds, introducing a rolling disturbance to the otherwise symmetric flight. The aircraft's response reflects the coupling between lateral–directional and longitudinal dynamics.

- **Longitudinal velocity (u):** The forward speed experiences a brief oscillation following the roll disturbance, but it quickly returns to a steady value near $115\text{--}120\text{ m/s}$. This small fluctuation arises from induced drag variations during the transient roll.
- **Lateral velocity (v):** A noticeable lateral deviation appears immediately after the aileron input, reaching about $\pm 1\text{ m/s}$. This is the expected response to a roll command that temporarily sideslips the aircraft.
- **Vertical velocity (w):** It exhibits a short transient similar to the base case but slightly amplified by the coupling with roll motion.

For the angular rates:

- **Roll rate (p)** shows a sharp spike right after the aileron input, representing the aircraft's roll acceleration, followed by a damped decay as the control returns to neutral.
- **Yaw rate (r)** becomes negative due to adverse yaw, a typical response in which the aircraft yaws opposite to the rolling direction before stabilizing.
- **Pitch rate (q)** is only slightly affected, showing minor oscillations as the roll–yaw coupling dissipates.

Finally, for the Euler angles:

- ϕ (roll angle) decreases sharply and stabilizes near a small negative value, confirming a short bank to one side.
- θ (pitch angle) undergoes minor oscillations, consistent with coupled longitudinal effects.
- ψ (yaw angle) shows a gradual drift, indicating a small heading change due to the roll–yaw coupling during recovery.

Case 3 — Left engine failure.

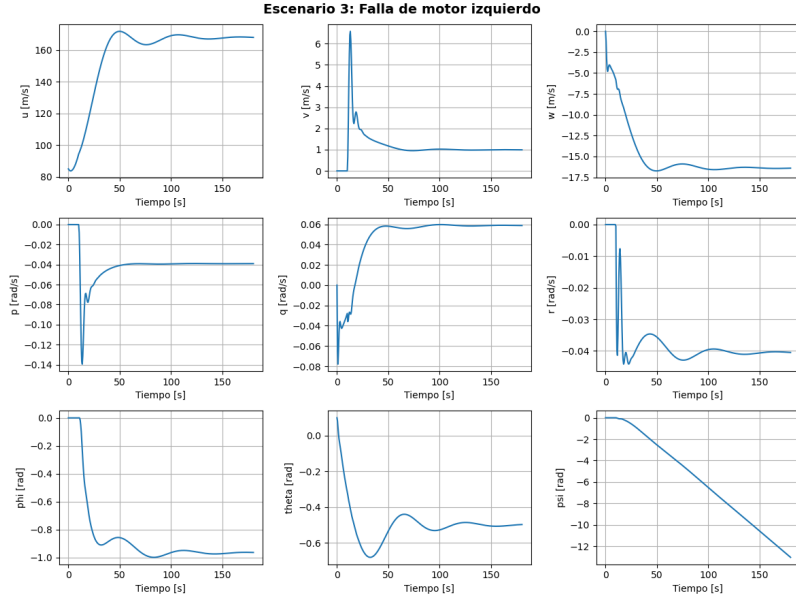


Figure 3: Case 3: Left engine failure at 10 s.

In this scenario, the left engine is shut down at $t = 10$ s, producing a strong asymmetric thrust condition. The resulting dynamics clearly show the coupling between longitudinal, lateral, and directional motion as the aircraft reacts to the unbalanced forces.

- **Longitudinal velocity (u):** Immediately after the engine failure, the total thrust decreases, but due to the asymmetric configuration, the aircraft accelerates briefly before gradually stabilizing around 160 m/s. This overshoot occurs as the right engine compensates and aerodynamic drag increases to balance thrust.
- **Lateral velocity (v):** A significant positive lateral component appears (around 5–6 m/s), reflecting the yawing motion induced by the loss of thrust on one side. This steady sideslip is a typical characteristic of engine-out asymmetric flight.
- **Vertical velocity (w):** The aircraft descends more steeply compared to previous cases, indicating a loss of lift and increased sink rate while the control system attempts to stabilize the attitude.

For the angular rates:

- **Roll rate (p)** shows a sharp negative spike, representing the roll moment caused by the asymmetric thrust from the right engine.
- **Pitch rate (q)** presents small oscillations as the aircraft adjusts its angle of attack to counter the new equilibrium.
- **Yaw rate (r)** becomes strongly negative, confirming that the aircraft yaws toward the inoperative engine, as expected from the asymmetric torque.

Finally, for the Euler angles:

- ϕ (roll angle) becomes notably negative, stabilizing near -1 rad, indicating a permanent bank toward the failed engine.
- θ (pitch angle) decreases sharply before oscillating and settling at a lower attitude, consistent with the descent observed in w .
- ψ (yaw angle) continuously decreases, showing a progressive heading deviation due to the persistent yawing moment.

Case 5 — Trim Search using Particle Swarm Optimization (PSO)

To determine the aircraft's steady-state trim condition, a Particle Swarm Optimization (PSO) algorithm was implemented. The goal of this procedure is to find the set of state and control variables that minimize the dynamic accelerations, ensuring the aircraft remains in equilibrium at a target airspeed of approximately 85 m/s.

Decision variables. The optimization vector

$$\mathbf{z} = [u, v, w, \phi, \theta, \delta_a, \delta_e, \delta_r, t]$$

contains both state components and control inputs, bounded within realistic aerodynamic and control limits. These variables define the body velocity components, attitude angles, control surface deflections, and throttle setting for both engines.

Cost function. The cost function $J(\mathbf{z})$ measures how far a given state-control pair (X, U) is from true equilibrium. It is defined as a weighted quadratic sum of normalized errors:

$$J = w_{\text{acc}} \sum_i \left(\frac{\dot{x}_i}{s_i} \right)^2 + w_{\text{ang}} \sum_i \left(\frac{\dot{\omega}_i}{s_i} \right)^2 + w_{V_a} \left(\frac{V_a - 85}{s_{V_a}} \right)^2 + w_{\text{lat}} \left(\frac{v}{s_v} \right)^2 + w_{\text{roll}} \left(\frac{\phi}{s_\phi} \right)^2 + w_{\text{cmd}} \sum_j \left(\frac{u_j}{s_{\text{cmd}}} \right)^2.$$

Each term penalizes deviations from the desired steady flight conditions:

- The first two groups ($w_{\text{acc}}, w_{\text{ang}}$) minimize translational and rotational accelerations, driving the system toward equilibrium.
- The third term enforces a target airspeed $V_a = 85$ m/s.
- The lateral and roll terms ($w_{\text{lat}}, w_{\text{roll}}$) penalize sideslip and roll angle to maintain coordinated, level flight.
- The command regularization term (w_{cmd}) prevents unrealistic control surface deflections, promoting physically consistent solutions.

Optimization algorithm. The PSO algorithm evolves a population of $N_p = 40$ particles, each representing a candidate solution \mathbf{z} , over 120 iterations. Particle velocities and positions are updated dynamically through an exploration-to-exploitation schedule:

$$\mathbf{v}_i \leftarrow w \mathbf{v}_i + c_1 r_1 (\mathbf{p}_i - \mathbf{x}_i) + c_2 r_2 (\mathbf{g} - \mathbf{x}_i),$$

where w is the inertia factor (decreasing from 0.9 to 0.4), and c_1, c_2 are cognitive and social coefficients that evolve from exploration to convergence.

At each iteration, the best individual (\mathbf{p}_i) and global (\mathbf{g}) solutions are updated based on the minimum cost J . The algorithm stops once the cost converges to a small value, indicating that aerodynamic, gravitational, and thrust forces are in balance.

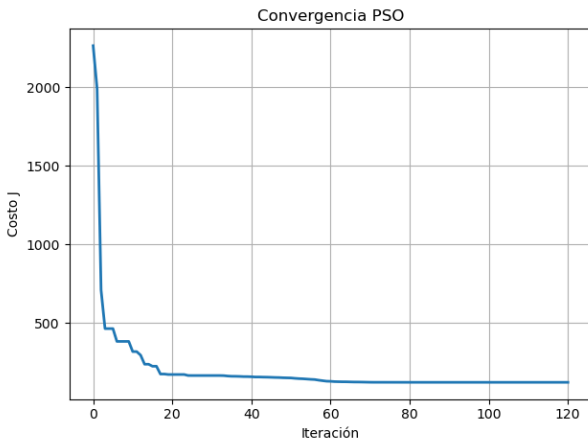


Figure 4: PSO Convergence History.

The optimization successfully converged to the following trim condition:

$$J^* = 121.586897$$

$$X_{\text{trim}} = \begin{bmatrix} 85.03 & -3.8 \times 10^{-6} & 0.36 & 0 & 0 & 0 & -4.26 \times 10^{-7} & 0.1745 & 0 \end{bmatrix}$$

$$U_{\text{trim}} = \begin{bmatrix} -1.71 \times 10^{-6} & -0.123 & -1.72 \times 10^{-6} & 0.167 & 0.167 \end{bmatrix}$$

These results indicate a stable equilibrium flight at approximately $V_a = 85$ m/s, with negligible sideslip ($v \approx 0$) and level roll attitude ($\phi \approx 0$). The small positive pitch angle $\theta \approx 0.1745$ rad ($\approx 10^\circ$) corresponds to the nose-up attitude required to generate lift equal to weight. The elevator deflection $\delta_e \approx -0.123$ rad ($\approx -7^\circ$) compensates for the pitching moment, while the throttle setting $t \approx 0.167$ per engine maintains the necessary thrust for steady level flight.